

Tunneling ionization in the multiphoton regime

G. Gibson, T. S. Luk, and C. K. Rhodes

*Laboratory for Atomic, Molecular, and Radiation Physics, Department of Physics,
University of Illinois at Chicago, P.O. Box 4348, Chicago, Illinois 60680*

(Received 12 January 1990)

Data on the threshold ionization intensities of rare-gas atoms with 248-nm irradiation in the 10^{13} – 10^{16} -W/cm² range of intensity are presented in the context of models involving tunneling ionization. Comparison is also made with the full Keldysh theory. It is shown that, although the experimental conditions fall well outside the tunneling regime as defined by the Keldysh theory, these relatively simple pictures accurately predict the threshold ionization intensities observed under the conditions studied. The main deviation of these results from the Keldysh theory occurs for the heavier elements at high charge states.

In the rapidly developing field concerning the study of high-intensity laser interactions with matter, there is now a wealth of data on the collision-free multiphoton ionization of the rare gases.^{1–4} Complementing these data are a variety of theories, at different levels of complexity, that can be used to explain the measured ionization rates.^{5–11} Two regimes are generally distinguished by the “Keldysh parameter,”⁵ $\gamma \equiv [(\text{ionization potential})/2 \times (\text{ponderomotive potential})]^{1/2}$: the multiphoton regime, where $\gamma \gg 1$ and the tunneling regime where $\gamma \ll 1$. Most experiments on multiphoton ionization of the rare gases are in the multiphoton regime,^{2–4} and complex theories^{5–7} have been developed to understand this case. The purpose of this article is to present a new analysis of data on the threshold ionization intensities of the rare gases obtained with subpicosecond 248-nm irradiation in the context to tunneling ionization models.^{1,8–11} Although the above definition of tunneling versus multiphoton ionization clearly places these experiments in the multiphoton regime, as γ ranges from about 1 to 8, the results demonstrate that relatively simple pictures involving tunneling ionization agree well with the measured threshold ionization intensities of the rare gases in the 10^{13} – 10^{16} -W/cm² range of intensity. In addition, we will compare the various levels of approximation typically used in these treatments.

The laser used in these experiments was a KrF* system amplifying a 500-fsec seed pulse up to an energy of approximately 20 mJ.¹² This radiation was focused into a vacuum chamber containing the target gas and the ions were detected with a standard time-of-flight spectrometer.¹³ The largest experimental uncertainty in the data is in the value of the threshold intensity. Not only is the focused intensity a difficult quantity to measure, there is a question as to how to define an intensity which is varying in space. Consider the focus of a flat-top beam. The spot size of the beam is generally taken to be the diameter at which the Bessel function describing the intensity distribution at the focus goes to its first zero. The average intensity of the field is then determined by the power in the beam divided by the area of the focal spot. However, the

peak intensity will be 3.67 times this value.¹⁴ Nevertheless, the average intensity is usually quoted in experimental work. While this may seem to be the appropriate quantity, the ionization rates generally increase rapidly with intensity, and thus the peak value of the focused intensity may be the relevant quantity. Most theories, of course, do not have this problem of definition, as a constant intensity is assumed. Clearly, in comparing experimental threshold intensities to theory, in the ideal case, one should average the calculated ionization rates throughout the focal volume.² This procedure is quite difficult, as the spatial characteristics of the focus are generally poorly known, and is rarely done. Consequently, for our analysis we will assume that the peak intensity is the significant physical parameter and thus multiply our average intensities by 3.67 for comparison with theoretical predictions. Given this definition of the threshold intensity, the uncertainty in the absolute experimental value is estimated to be a factor of 5.¹⁵ From data taken with mixed gases, and comparing charge states, the relative uncertainty is estimated to be reduced to a factor of 2.

Figure 1(a) presents the experimental data on the threshold ionization intensities of the rare gases with 248-nm irradiation.¹⁵ Clearly, a meaningful statement of a threshold intensity requires some discussion of the ionization rate defining the threshold of observation. In these experiments the ionization rate at threshold is estimated¹⁵ to be 2×10^9 sec⁻¹. However, for all the models considered, calculations show that a factor of 2 change in intensity either way around the threshold value changes the ionization rate by at least two orders of magnitude. Thus it is not necessary to know the threshold ionization rate to high accuracy.

Two important features in Fig. 1(a) are readily apparent: first, there is no obvious functional dependence of the threshold ionization intensity I_{th} on the ionization potential E_p , and second, there is a systematic lowering of I_{th} with increasing atomic number. These two salient characteristics have been basic aspects of the data on

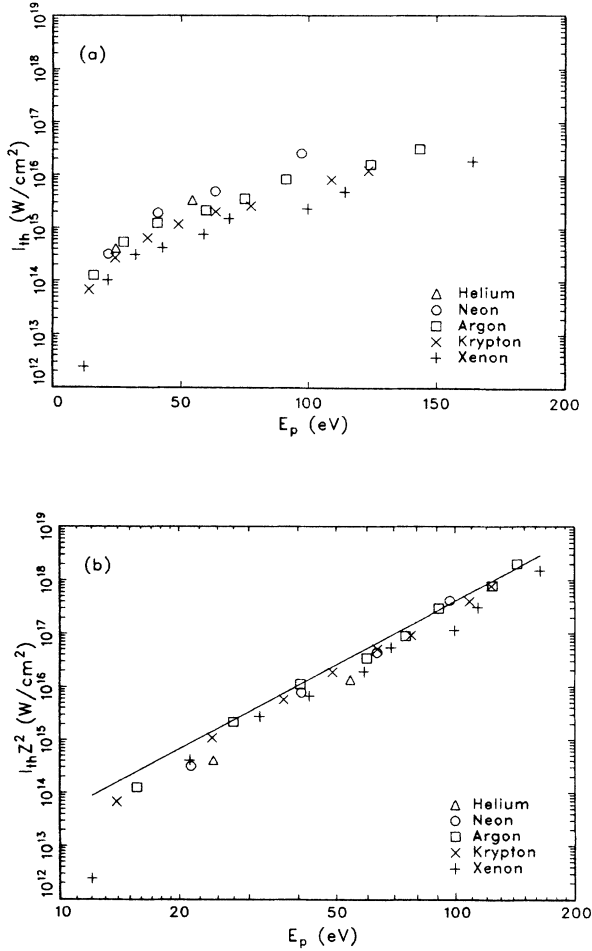


FIG. 1. (a) Threshold ionization intensities of the rare gases with subpicosecond 248-nm irradiation. (b) Same data replotted with Eq. (1) to show the scaling relationships. All intensities are peak values. (See Fig. 2 for uncertainty in the intensities.)

multiphoton ionization from some of the earliest observations¹⁶ of these processes.

The simplest model of tunneling ionization consists of a one-dimensional (1D) Coulomb potential.¹ In an external, static electric field, an electron in this 1D atom “sees” a finite potential barrier to ionization whose width and height depends on the strength of the field. The threshold intensity for ionization I_{th} is defined as the intensity at which the potential barrier is reduced to the ionization potential of the atom. The result of this calculation is¹

$$I_{th} = cE_p^4 / 128\pi e^6 Z^2, \quad (1)$$

where E_p is the ionization potential, Z the charge of the resulting ion, c the speed of light, and e the charge of an electron.

This model has two defects which partially cancel each other, resulting in a fairly accurate prediction of I_{th} . First, when the barrier is lowered to the ionization potential, the barrier is completely removed, producing ionization rates characteristic of atomic time scales ($\sim 10^{16} \text{ sec}^{-1}$). These rates are much higher than the threshold rates, and thus overestimate the values for the threshold ionization intensities. In contrast to the one-dimensional picture, in three dimensions the lowering of the potential barrier to the ionization potential, at the intensity given by Eq. (1), will occur in only one direction in space. In every other direction the potential barrier will be higher, leading to an underestimation of the threshold ionization intensity. However, despite these differences, Eq. (1) does reveal two important scaling relationships. First, besides E_p , I_{th} also depends on Z^2 . This scaling can be accounted for by simply considering the variable $I_{th} Z^2$, as will be done throughout the rest of this discussion. Second, $I_{th} Z^2$ is proportional to E_p^4 . Clearly, a log-log plot of $I_{th} Z^2$ versus E_p should exhibit these basic scaling relationships and Fig. 1(b) shows such a representation for the data in Fig. 1(a). The data now fall almost perfectly on a straight line with a slope of 4, and the systematic dependence on atomic number has been largely removed. Furthermore, Eq. (1) predicts quite well the threshold ionization intensities over five orders of magnitude in the parameter $I_{th} Z^2$. However, the results of Eq. (1) are consistently too high and there remains a more complex dependence on atomic number.

A more refined model than represented by Eq. (1) involves a three-dimensional atom and a calculation of the tunneling rate through the potential barrier at an arbitrary intensity.^{8,9,17} The resulting ionization rate for a static electric field from this model is¹⁷

$$W_{st}(E_s) = 4\omega_0(2E_p)^{5/2} E_s^{-1} \exp[-\frac{2}{3}(2E_p)^{3/2} E_s^{-1}] \quad (2)$$

for $(2E_p)^{3/2} \gg E_s$, where E_s is the static field in atomic units (e/a_0^2), E_p the ionization potential in atomic units (e^2/a_0), and ω_0 the atomic unit of frequency ($4.1 \times 10^{16} \text{ sec}^{-1}$). To calculate the ionization rate in an optical field, Eq. (2) can be time averaged over one cycle of the field. This time average can be done exactly in terms of the K_0 modified Bessel function.¹⁸ However, in the limit $(2E_p)^{3/2} \gg E_s$, this time average goes over to a simpler form:¹⁰

$$W_{ac} = (3/\pi)^{1/2} E^{1/2} (2E_p)^{-3/4} W_{st}(E), \quad (3)$$

where E is the peak of the alternating field in atomic units.

Equation (3) can be further improved to include nonhydrogenic systems. The static ionization rate in this orbital picture is given by^{10,11}

$$W_{st} = \omega_0 C_n^2 * I E_p \frac{(2l+1)(l+|m|)!}{2^{|m|} (|m|)! (l-|m|)!} [2(2E_p)^{3/2} E^{-1}]^{2n* - |m| - 1} \exp[-\frac{2}{3}(2E_p)^{3/2} E^{-1}], \quad (4)$$

where n^* is the effective principle quantum number [$n^* = Z(2E_p)^{-1/2}$], l the orbital angular quantum number, and m the magnetic quantum number. C_{n^*l} is a numerical constant on the order of 2. The approximate time average of Eq. (4) is also given by Eq. (3).

The last model that we consider is the well-known Kel-

dysch theory.⁵ As the γ parameter is in the intermediate regime, $1 < \gamma < 8$, a limiting form of the theory could not be used. Thus, we evaluated the full form as presented in Ref. 2, but do not reproduce these expressions here.

Figures 2(a)–2(e) show the results of the four models represented by Eq. (1), Eq. (3) using the static ionization

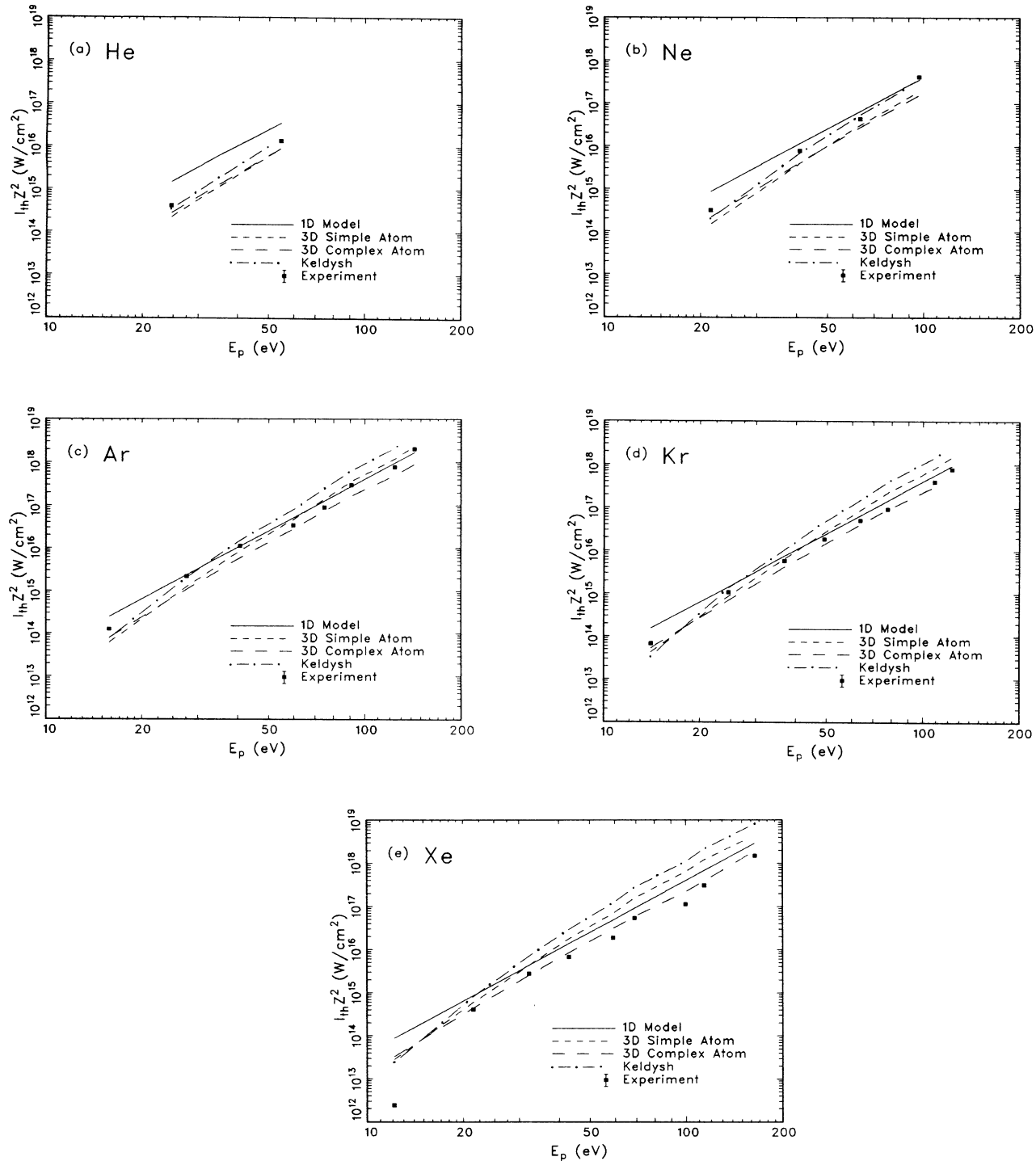


FIG. 2. Threshold ionization intensities for the rare gases from Fig. 1 along with calculated results from various theories. The 1D model corresponds to Eq. (1), the 3D simple atom to Eqs. (2) and (3), and the 3D complex atom to Eqs. (3) and (4). The Keldysh line was calculated from the equations in Ref. 2. All intensities are peak values. The relative uncertainty in the intensities is indicated by an error bar in the legend.

rates for the hydrogenic and nonhydrogenic systems, and the Keldysh theory, with the experimental data from Fig. 1 for the rare gases. Several interesting features are apparent. First, the 3D simple atom picture and the Keldysh theory both agree well with the experimental data for the light elements, helium and neon. However, they both get consistently worse for the heavier atoms at the higher charge states. This trend makes sense, as both models assume exact hydrogenic potentials, a poor approximation for the heavier gases. Second, as noted above, the 1D model uniformly gives too high a threshold intensity and tends to be the worst for the neutral species. Third, the 3D complex model, expressed by Eq. (4), consistently gives good results over the entire range of atomic number and charge state studied. Fourth, the one point which deviates considerably from any model is the threshold ionization of neutral xenon. However, this is clearly a case of multiphoton ionization, as there is a very close two-photon resonance ($5p \rightarrow 6p$) with 248-nm radiation. The multiphoton regime can be characterized by being very sensitive to the specific atomic structure, particularly near exact resonances.

The three tunneling models considered here are all quasistatic theories, in other words, γ is vanishingly small. However, as mentioned above, the data were taken in a regime where γ is greater than 1. Although a full tunneling ionization model for a Coulomb potential and an arbitrary γ has been solved¹⁰ it is quite complicated. Considering a δ -function potential results in a somewhat simpler expression for the ionization rate,¹⁰ and from this model we estimate the effect of varying γ on the threshold intensities. The result is that up to a value of $\gamma=3$

the threshold intensities decrease by less than a factor of 2.

Measuring threshold ionization intensities is a relatively simple experiment and the results are insensitive to the actual ionization rates. Theoretical threshold values are insensitive to the details of a given model for the same reason. Thus it is difficult to use threshold data to evaluate the merits of various theories unless very precise measurements are made. On the other hand, measuring threshold intensities provides an easy method of determining focused intensities to a reasonable accuracy.

There are three main conclusions. First, even using 248-nm irradiation, threshold ionization intensities can be accurately predicted by relatively simple tunneling ionization models. Second, while a 1D Coulomb potential model correctly gives the basic scaling laws for tunneling ionization, a 3D complex atom picture is required to give uniformly better quantitative agreement over the entire range of gases and charge states studied. Third, threshold ionization intensities are rather insensitive to the details of the theoretical models and thus have limited usefulness in testing ionization models. Finally, we note that with the use of intensities in excess of 10^{18} W/cm², which are now achievable, it will be possible, based on extrapolating Eq. (1), to remove completely the $4d$ shell from xenon producing kryptonlike Xe¹⁸⁺.

The authors would like to acknowledge fruitful conversations with A. Szöke and M. Perry. Support for this research was provided by the U.S. Air Force Office of Scientific Research, the U.S. Office of Naval Research, and the Strategic Defense Initiative Organization.

¹S. August, D. Strickland, D. D. Meyerhofer, S. L. Chin, and J. H. Eberly, *Phys. Rev. Lett.* **63**, 2212 (1989).

²M. D. Perry, O. Landen, A. Szöke, and E. M. Campbell, *Phys. Rev. A* **37**, 747 (1988).

³A. L'Huillier, L. A. Lompré, G. Mainfray, and C. Manus, *J. Phys. B* **16**, 1363 (1983).

⁴S. L. Chin, C. Rolland, P. B. Corkum, and P. Kelly, *Phys. Rev. Lett.* **61**, 153 (1988).

⁵L. V. Keldysh, *Zh. Eksp. Teor. Fiz.* **47**, 1945 (1964) [*Sov. Phys.—JETP* **20**, 1307 (1965)].

⁶R. M. Potvliege and Robin Shakeshaft, *Phys. Rev. A* **38**, 4597 (1988).

⁷H. Reiss, *Phys. Rev. A* **22**, 1786 (1980).

⁸L. D. Landau and E. M. Lifshitz, *Quantum Mechanics*, 3rd ed. (Pergamon, London, 1978).

⁹B. M. Smirnov and M. I. Chibisov, *Zh. Eksp. Teor. Fiz.* **49**, 841 (1965) [*Sov. Phys.—JETP* **22**, 585 (1966)].

¹⁰A. M. Perelomov, V. S. Popov, and M. V. Terent'ev, *Zh. Eksp. Teor. Fiz.* **50**, 1393 (1966) [*Sov. Phys.—JETP* **23**, 924 (1966)].

¹¹M. V. Ammosov, N. B. Delone, and V. P. Krainov, *Zh. Eksp. Teor. Fiz.* **64**, 2008 (1986) [*Sov. Phys.—JETP* **64**, 1191

(1986)].

¹²A. P. Schwarzenbach, T. S. Luk, I. A. McIntyre, U. Johann, A. McPherson, K. Boyer, and C. K. Rhodes, *Opt. Lett.* **11**, 499 (1986).

¹³T. S. Luk, U. Johann, H. Egger, H. Pummer, and C. K. Rhodes, *Phys. Rev. A* **32**, 214 (1985).

¹⁴M. Born and E. Wolf, *Principles of Optics* (Pergamon, New York, 1980).

¹⁵U. Johann, T. S. Luk, I. A. McIntyre, A. McPherson, A. P. Schwarzenbach, K. Boyer, and C. K. Rhodes, in *Short Wavelength Coherent Radiation: Generation and Applications, Monterey, California, 1986*, Proceedings of the Topical Meeting on Short Wavelength Coherent Radiation, AIP Conf. Proc. No. 147, edited by D. Atwood and J. Bokor (AIP, New York, 1986) p. 202.

¹⁶T. S. Luk, H. Pummer, K. Boyer, M. Shahidi, H. Egger, and C. K. Rhodes, *Phys. Rev. Lett.* **51**, 110 (1983).

¹⁷N. H. Burnett and P. B. Corkum, *J. Opt. Soc. Am. B* **6**, 1195 (1989).

¹⁸I. S. Gradshteyn and I. M. Ryzhik, *Tables of Integrals, Series, and Products* (Academic, New York, 1965).